Progress In Electromagnetics Research, PIER 77, 149–170, 2007

A NOVEL PROPOSAL FOR ULTRA-HIGH RESOLUTION AND COMPACT OPTICAL DISPLACEMENT SENSOR BASED ON ELECTROMAGNETICALLY INDUCED TRANSPARENCY IN RING RESONATOR

R. Yadipour, K. Abbasian, A. Rostami and Z. D. Koozehkanani

Photonics and Nanocrystals Research Lab. (PNRL)
Faculty of Electrical and Computer Engineering
University of Tabriz
Tabriz 51664, Iran

Abstract—In this paper a novel method for ultra-high-resolution, compact and tunable optical displacement sensor using ring resonator and electromagnetically induced transparency (EIT) is proposed. The introduced technique uses ring resonator as an interesting element including high quality factor. We show that the proposed sensor can easily detect well below nanometer ranges. It is shown that the proposed idea of using EIT the resolution of the sensor is so high for displacement below mm range and for ranges larger than mm the sensitivity of the proposed sensor in both EIT and traditional cases is same approximately. Also, the proposed sensor is optically tunable. So, depends on required resolution optical control field can be used to tune the sensitivity of the proposed device.

1. INTRODUCTION

Optical method for computing and processing of engineering problems is one of best alternatives. Optical techniques have been extended in communication especially fiber based networks. Recently making and introducing building blocks to realize basic backbone for computing is main industry and science request. Also, combination of optical and mechanical systems named optomechatronics or optical micro electromechanical systems (optical-MEMS) opened new insight to device design for making processing blocks. Also, design strategy based on optical-MEMS is suitable approach for sensor design too. For

realization of ultra high precision systems in deep sub-micron or nano-scales one of important sensors is displacement sensing. For realization of high precision displacement sensor different methods have been used. Here we are going to review some of them and investigate advantages and disadvantages of them.

One of the presented displacement sensor was discussed in [1]. The presented method used variable resistance as physical phenomenon for detection of the object displacement. In this work object changed the position of the 3rd terminal of the variable resistor and the total resistance is changed. It is obvious that small displacement can't be measured.

The second method is based on change of air gap in transformer [1]. Variation of the air gap introduces variable induced voltage. Measuring of the induced potential is criteria of the object displacement. According previous method this approach can't be so sensitive in displacement measurement.

Advanced version of the second method for displacement measurement is linear variable differential transformer (LVDT) [1]. This type of displacement sensors cover sub-micron to mm range of operation. So, for ultra high precision measurement can't be used.

Another related sensor for displacement measurement was done using capacitance measuring which is presented and discussed in [1]. In this method object displacement changes the capacitance coefficient of the capacitor and using this variation the displacement can be estimated.

Piezoelectric material also can be used to measure the displacement of the object [1]. This effect refers to the fact that applied mechanical pressure due to object displacement causes an induced voltage which is corresponding to the object displacement.

Ultrasound method is another interesting approach for displacement monitoring. In this method ultrasound pulses applied to the object and backward wave is detected. Based on forward transmitting and backward receiving waves the object displacement is calculated [1]. Since the wavelength of the ultrasound wave is high enough, so precision of the displacement measurement is low.

Optical method is another important technique for displacement measurement. These approaches were discussed in [2–4]. In this method two basic techniques are used. One of these methods based on the reflected back intensity. In this technique variation of displacement converted to the level of intensity measured with high resolution photodetectors. Interference of the forward and backward traveling waves and phase difference is criteria of the displacement measurement. In these methods resolution of the displacement can be increased to

near Pico meter. In these sensors range of operation usually limited to micro meter range.

Another interesting method developed recently is based on ring resonators and used for high resolution displacement measurement [5]. In this method usually a narrow gap is made on top part of the ring and outgoing wave from this gap impact on object and reflected back to the ring. On the other hand object and ring simultaneously introduce a resonant cavity. Displacement of the object changes the oscillation and resonance frequency of the system. So, measuring of the output intensity for input light at given wavelength is used for measurement of the displacement.

Ring resonator is a basic and important device which is used recently more [6–24]. Also, it is a basic cell for making all optical system. So it is important to apply this device to displacement measurement. There is a basic problem with ring resonator. It is wide spectral shape which causes low precision in displacement measurement. For this purpose in this paper we present a new idea for improving this problem. Our method is based on doping of ring resonator with 3-level atoms or nanocrystals. In this situation the spectral profile of the ring resonators is decreased strongly and thus the precision of the sensor is increased. For this proposal we use from quantum optical effects applied to describe of the nanocrystals [25]. In this proposal we used 3-level atoms with given density. First we calculate the optical susceptibility and then using control field changing of the obtained susceptibility is controlled. Obtained optical susceptibility is used for management of the guided wave and finally optical output intensity is extracted. Since obtained optical susceptibility determine the resonance frequency, so applied light in a given wavelength may have different output intensity in the output port. So, ultra small narrowband spectral profile can be used for obtaining on-off behavior in the output for small displacement. We show that our proposed method can measure well below nanometer range.

Organization of the paper is as follows.

In Section 2 mathematical background is explained. Simulation results is illustrated and discussed in Section 3. Finally the paper ends with a short conclusion.

2. MATHEMATICAL BACKGROUND

The proposed structure for ultra-high resolution displacement sensor is illustrated in Fig. 1. It is shown that the proposed structure includes a main waveguide coupled to single ring resonator. Top part of the

ring resonator is closed by light propagation and reflection though clean surface of the moving object in which distance between object and ring should be measured. By variation of the distance of the object the resonance frequency of the ring resonator is changed and the output intensity is comes down and can be measured to evaluate the unknown distance. Now, in the following, we first model the light propagation through this complex system and then using doping of the 3-level particles inside ring (nanocrystal), we try to obtain the ultra narrow transfer function to increase the resolution of the sensor.

First we consider normal (without EIT) ring resonator in the following structure form.

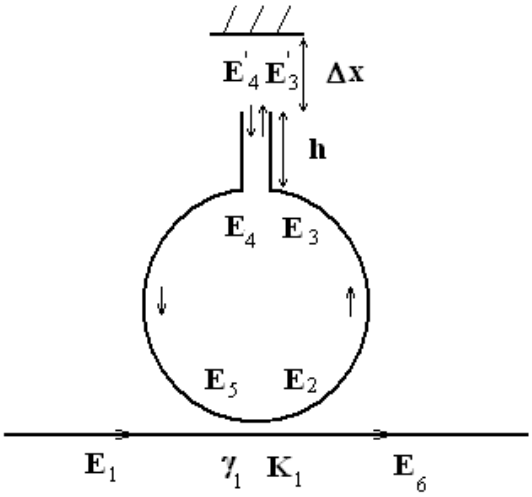

Figure 1. Schematic of the high-resolution displacement sensor.

According to light propagation in linear and isotropic media the following relations are presented to describe the illustrated coupler input-output functions.

$$E_6 = \sqrt{1-\gamma_1} \cdot \left[\sqrt{1-K_1} \cdot E_1 - j\sqrt{K_1} \cdot E_5\right], \quad (1)$$

$$E_2 = \sqrt{1-\gamma_1} \cdot \left[\sqrt{1-K_1} \cdot E_5 - j\sqrt{K_1} \cdot E_1\right], \quad (2)$$

where γ_1 and K_1 are Coupler's loss and the coupling coefficient respectively. Using the wave propagation inside ring resonator, two aligned waveguide ends, free space parts and reflection from sample

surface, we have

$$E_3 = E_2 \exp\left(\frac{-\alpha \cdot L_{23}}{2}\right) \exp\left(-j\beta \cdot L_{23}\right), \tag{3}$$

$$E_3' = E_3 \exp\left(\frac{-\alpha \cdot h}{2}\right) \exp\left(-j\beta \cdot h\right), \tag{4}$$

$$E_4' = r \cdot E_3' \exp\left(\frac{-\alpha_0 \cdot \Delta x}{2}\right) \exp\left(-j\beta_0 \cdot 2\Delta x\right), \tag{5}$$

$$E_4 = E_4' \exp\left(\frac{-\alpha \cdot h}{2}\right) \exp\left(-j\beta \cdot h\right), \tag{6}$$

$$E_5 = E_4 \exp\left(\frac{-\alpha \cdot L_{45}}{2}\right) \exp\left(-j\beta \cdot L_{45}\right), \tag{7}$$

where α and β are the ring (and fiber) loss coefficient and wave propagation vector respectively. Also, α_0 and β_0 are loss and wave vector of free space respectively too. The appeared L_{23} and L_{45} parameters are lengths of two parts of the ring resonator. Also, h and Δx are fiber and free space lengths as illustrated in Fig. 1 respectively. Finally r is the reflection coefficient of the reflecting surface of the object.

After some mathematical manipulation the following transfer function is obtained as follows. This equation can be used for evaluation of the normal ring resonator based optical displacement sensor.

$$\frac{E_6}{E_1} = \frac{\sqrt{(1-\gamma_1)(1-K_1)} - \left[(1-\gamma_1) \cdot r \cdot e^{\frac{-\alpha \cdot L_{23}}{2}} \cdot e^{\frac{-j\beta \cdot L_{23}}{2}} \cdot e^{-\alpha \cdot h} \cdot e^{-j2\beta \cdot h} \cdot e^{-\alpha_0 \cdot \Delta x} \cdot e^{-j2\beta_0 \cdot \Delta x} \cdot e^{\frac{-\alpha \cdot L_{453}}{2}} \cdot e^{-j\beta \cdot L_{45}}\right]}{1 - \left[\sqrt{(1-\gamma_1)(1-K_1)} \cdot r \cdot e^{\frac{-\alpha \cdot L_{23}}{2}} \cdot e^{\frac{-j\beta \cdot L_{23}}{2}} \cdot e^{-\alpha \cdot h} \cdot e^{-j2\beta \cdot h} \cdot e^{-\alpha_0 \cdot \Delta x} \cdot e^{-j2\beta_0 \cdot \Delta x} \cdot e^{\frac{-\alpha \cdot L_{453}}{2}} \cdot e^{-j\beta \cdot L_{45}}\right]} \tag{8}$$

Now, we are going to develop mathematical method to describe effect of 3-level particles doped into ring resonator on characteristics of designed displacement sensor. Using suitable 3-level particles in ring resonator, which can be realized using quantum dots, we show that the resolution of the proposed sensor can be increased and tuned optically. Fig. 2 shows the model of 3-level particles including probe and control fields and decay rates. In the model the control and probe fields applied between levels 2 and 3 and levels 1 and 2 respectively. Due to applied electric field the optical characteristics is changed and in the following brief theoretical calculation for description of the system

performance is presented. After some mathematical manipulation the following matrix form of the Hamiltonian (Eq. (9)) and density matrix (Eq. (10)) are given as follows.

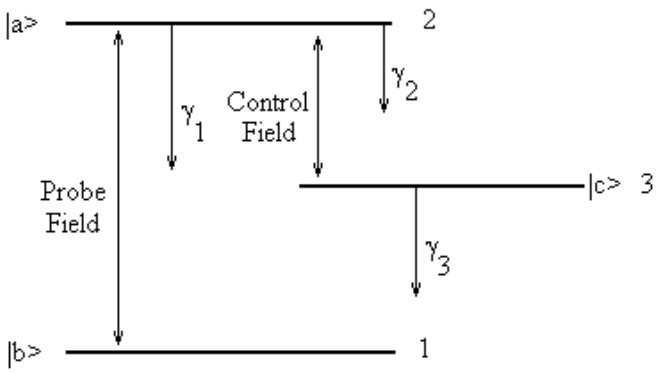

Figure 2. Schematic of 3-level particles.

$$\hat{H} = \begin{bmatrix} \omega_b & 0 & -\frac{\gamma_{ab}\varepsilon}{2\hbar}e^{i\upsilon t} \\ 0 & \omega_c & -\frac{1}{2}\Omega_\mu e^{i\phi_\mu}e^{i\upsilon_\mu t} \\ -\frac{\gamma_{ab}\varepsilon}{2\hbar}e^{-i\upsilon t} & -\frac{1}{2}\Omega_\mu e^{-i\phi_\mu}e^{-i\upsilon_\mu t} & \omega_a \end{bmatrix}, \qquad (9)$$

where ω_a, ω_b, ω_c, γ_{ab}, ε, υ, υ_μ, ϕ_μ and Ω_μ are frequencies corresponding to three levels, decay rate between levels a and b, amplitude of the control field, probe field frequency, control field frequency, control field phase and Rabi frequency of the control field respectively. In the following density matrix of the 3-level particles is presented.

$$\rho = \begin{bmatrix} \rho_{bb} & \tilde{\rho}^*_{cb}e^{i\omega_{cb}t} & \tilde{\rho}^*_{ab}e^{i\omega_{ab}t} \\ \tilde{\rho}_{cb}e^{-i\omega_{cb}t} & \rho_{cc} & \tilde{\rho}^*_{ac}e^{i\omega_{ac}t} \\ \tilde{\rho}_{ab}e^{-i\omega_{ab}t} & \tilde{\rho}_{ac}e^{-i\omega_{ac}t} & \rho_{aa} \end{bmatrix}, \qquad (10)$$

where ω_{cb}, ω_{ab} and ω_{ac} are frequencies corresponding to energies between levels in the presented model. Based on the time development equation of density matrix in the following differential equation is

given.

$$\dot{\tilde{\rho}}_{ab} = -(i\Delta + \gamma_1)\,\tilde{\rho}_{ab} + \frac{i}{2}\frac{\gamma_{ab}\varepsilon}{\hbar} + \frac{i}{2}\Omega_\mu e^{-i\Phi_\mu}\tilde{\rho}_{cb} \tag{11}$$

$$\dot{\tilde{\rho}}_{cb} = -(i\Delta + \gamma_3)\,\tilde{\rho}_{cb} + \frac{i}{2}\Omega_\mu e^{i\Phi_\mu}\tilde{\rho}_{ab} \tag{12}$$

where $\Delta = \omega_{ab} - \upsilon$ and $\upsilon_\mu = \omega_{ac}$ are frequency detuning and control field frequency respectively. Considering the following matrix,

$$M = \begin{bmatrix} \gamma_1 + i\Delta & -\dfrac{i}{2}\Omega_\mu e^{-i\Phi_\mu} \\ -\dfrac{i}{2}\Omega_\mu e^{i\Phi_\mu} & \gamma_3 + i\Delta \end{bmatrix}, \tag{13}$$

and basic mathematical formulation for optical susceptibility the following relation is given as

$$\chi_{ab} = -\frac{\gamma_{ab}^2}{i\varepsilon_0\hbar}M^{-1} \tag{14}$$

Also, the real and imaginary parts of optical susceptibility are given as

$$\chi' = -\frac{N_a\gamma_{ab}^2}{\varepsilon_0\hbar Z}\left[\gamma_3(\gamma_1+\gamma_3) + \left(\Delta^2 - \gamma_1\gamma_3 - \Omega_\mu^2/4\right)\right], \tag{15}$$

$$\chi'' = \frac{N_a\gamma_{ab}^2}{\varepsilon_0\hbar Z}\left[\Delta^2(\gamma_1+\gamma_3) - \gamma_3\left(\Delta^2 - \gamma_1\gamma_3 - \Omega_\mu^2/4\right)\right], \tag{16}$$

where $Z = \left(\Delta^2 - \gamma_1\gamma_2 - \Omega_\mu^2/4\right)^2 + \Delta^2(\gamma_1+\gamma_2)^2$ and N_a is density of nanocrystals.

Based on basic and fundamental relations between optical susceptibility and absorption coefficient and refractive index we have the following relations.

$$\alpha = \frac{\kappa}{2}\chi'', \quad \delta n = n\frac{\chi'}{2} \tag{17}$$

Finally the propagating wave vector in ring resonator doped with 3-level particles is given in the following.

$$\beta = \frac{\upsilon n}{c} \tag{18}$$

In the next section simulation results based on developed mathematical model are presented and discussed.

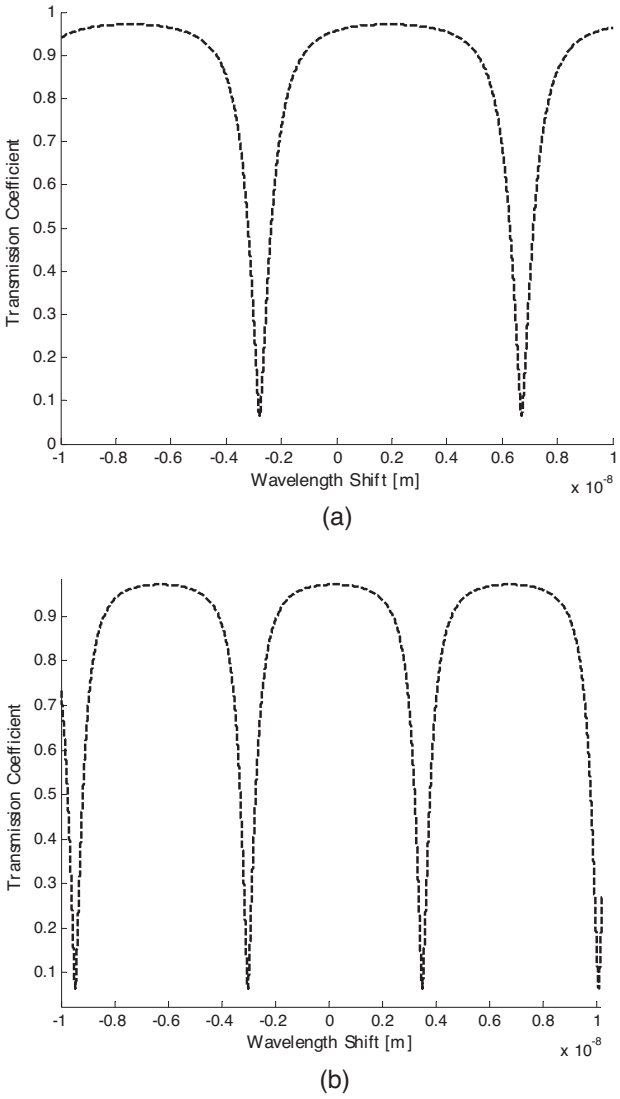

Figure 3. Transmission coefficient of optical displacement sensor based on ring resonator. (a) $1\,\mu$m displacement and (b) $5\,\mu$m displacement. $L_{23} = L_{45} = 48\,\mu$m, $h = 5\,\mu$m, $K_1 = 0.4$, $\lambda_0 = 1.55\,\mu$m, $r = 0.8$, $\gamma_1 = 10^{-3}\,\mathrm{m}^{-1}$, $\alpha = 10^{-3}\,\mathrm{m}^{-1}$, $\alpha_0 = 0.1\,\mathrm{m}^{-1}$. (a) $\Delta x = 1\,\mu$m, (b) $\Delta x = 5\,\mu$m.

3. SIMULATION RESULTS

In this section two cases are considered.

1. Normal case (ring resonator without 3-level doping)
2. EIT case (ring resonator with 3-level doping)

1. Normal case- In this case first, we consider a proposal for optical displacement sensor using ring resonator. Consider the structure illustrated in Fig. 1. For this structure the transmission coefficient versus differential wavelength is illustrated in Fig. 3. As it is shown in this case which part a and b are corresponds two typically different non-zero displacements respectively. It is observed that different displacements correspond to different resonance frequency.
2. EIT case- Now, typically effect of EIT on the transmission coefficient of the proposed structure is investigated. It is observed that the profile of the transmission coefficient in the case of EIT is so narrower than the transmission coefficient for normal case. It is interesting from displacement measurement point of view. In first part, real and imaginary parts of the optical susceptibility are illustrated.

Figure 4 shows effect of additional nanocrystal on the transmission coefficient of the proposed sensor. It is shown that in the case of doped 3-level particles the filtering behavior of the proposed structure is ultra sharp and narrowband. Thus small displacement introduces on-off switching of the transmission coefficient. Finally in this case ultra-high resolution is achievable.

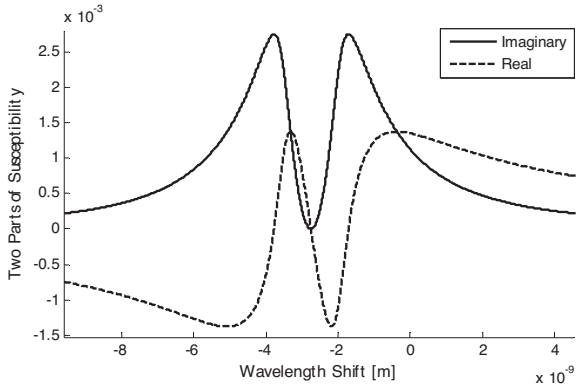

(a)

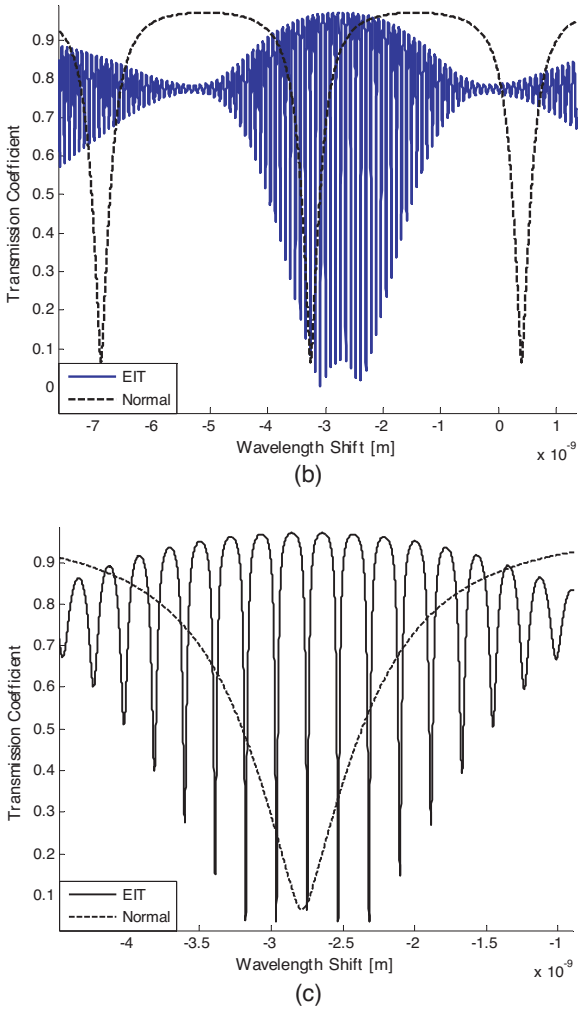

Figure 4. Transmission coefficient Vs. wavelength for normal and EIT cases in optical displacement sensor based on ring resonator. (a) Optical susceptibility, (b) Transmission coefficient for normal and EIT cases and (c) zoom in of the transmission coefficient in both cases. $L_{23} = L_{45} = 48\,\mu$m, $h = 5\,\mu$m, $\Delta x = 15\,\mu$m, $K_1 = 0.4$, $\lambda_0 = 1.55\,\mu$m, $r = 0.8$, $\gamma_1 = 10^{-3}\,\mathrm{m}^{-1}$, $\alpha = 10^{-3}\,\mathrm{m}^{-1}$, $\alpha_0 = 0.1\,\mathrm{m}^{-1}$, $E_{Control} = 2.5 \times 10^{13}\,\mathrm{Vm}^{-1}$, $\gamma_1 = 10^{13}$, $\gamma_2 = \gamma_3 = 10^8$, $\gamma_{ab} = 10^{-10}e$-cm, $N_a = 10^{23}\,\mathrm{cm}^{-3}$.

In the following effect of the control field on system performance is investigated. First we consider effect of control field on optical susceptibility. It is observed that with increasing of the control field slope of the linear part of the optical susceptibility in central part is decreased and minimum region of the imaginary part corresponding to central part is broadened. On the other hand with increasing of the control field transparency region is extended due to high level control field which introduces occupy excited level and the probe field in wide range can't be absorbed.

It is shown that with increasing of the control field the transparent region is extended and the slope of the real part of refractive index is decreased. Thus in wide frequency range of the input signal system is in transparent and oscillatory nature of the transmission coefficient is increased.

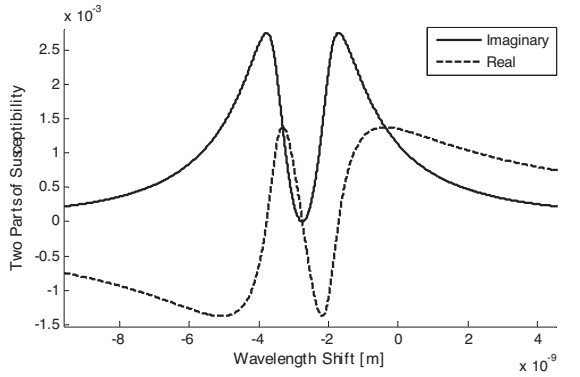

(a)

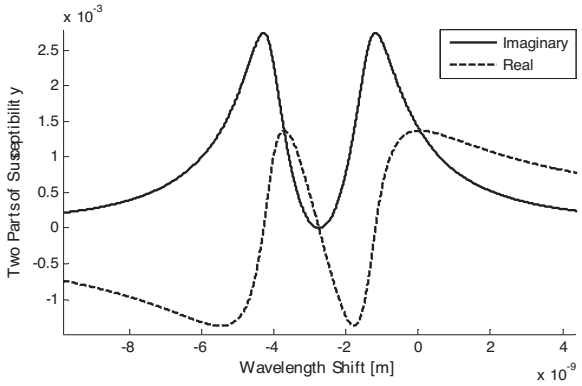

(b)

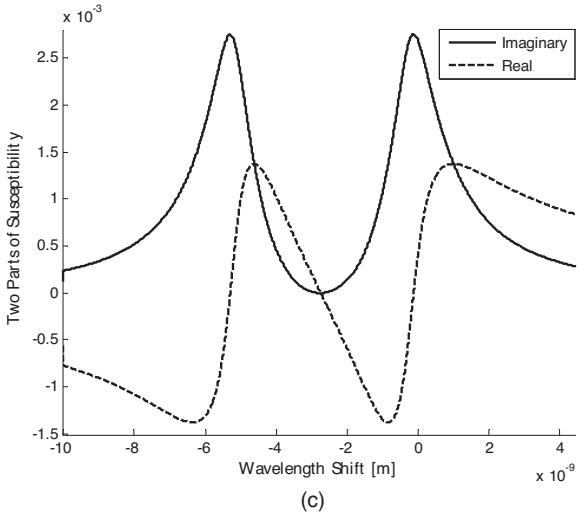

Figure 5. Optical susceptibility Vs. wavelength for different control field as parameter. $L_{23} = L_{45} = 48\,\mu$m, $h = 5\,\mu$m, $\Delta x = 15\,\mu$m, $K_1 = 0.4$, $r = 0.8$, $\gamma_1 = 10^{-3}\,\mathrm{m}^{-1}$, $\alpha = 10^{-3}\,\mathrm{m}^{-1}$, $\alpha_0 = 0.1\,\mathrm{m}^{-1}$, $\lambda_0 = 1.55\,\mu$m, $\gamma_1 = 10^{13}$, $\gamma_2 = \gamma_3 = 10^8$, $\gamma_{ab} = 10^{-10}e$-cm, $N_a = 10^{23}\,\mathrm{cm}^{-3}$. (a) $E_{Control} = 10^{13}\,\mathrm{Vm}^{-1}$, (b) $E_{Control} = 1.5 \times 10^{13}\,\mathrm{Vm}^{-1}$, (c) $E_{Control} = 2.5 \times 10^{13}\,\mathrm{Vm}^{-1}$.

Then for the mentioned above cases the transmission coefficient is illustrated and effect of the control field on this coefficient is shown in the following.

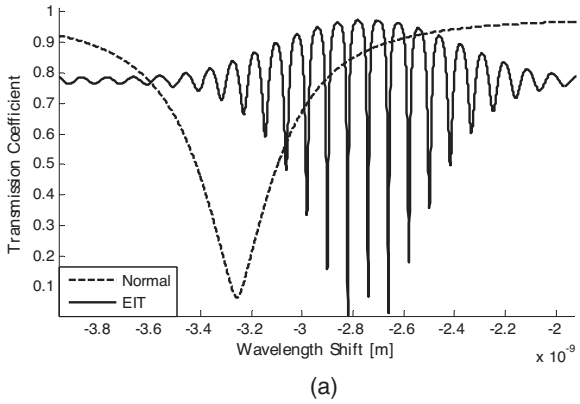

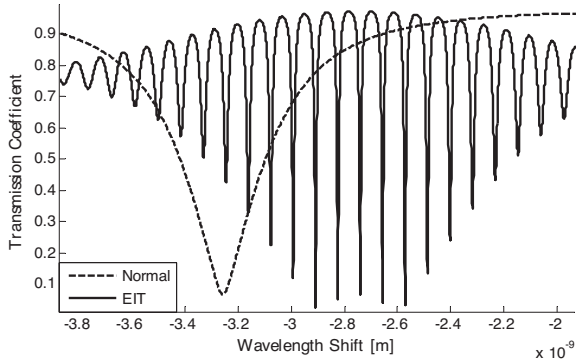

Figure 6. Transmission coefficient Vs. wavelength for normal and EIT cases of optical displacement sensor. $L_{23} = L_{45} = 48\,\mu$m, $h = 5\,\mu$m, $\Delta x = 15\,\mu$m, $K_1 = 0.4$, $r = 0.8$, $\gamma_1 = 10^{-3}\,\mathrm{m}^{-1}$, $\alpha = 10^{-3}\,\mathrm{m}^{-1}$, $\alpha_0 = 0.1\,\mathrm{m}^{-1}$, $\lambda_0 = 1.55\,\mu$m, $\gamma_1 = 10^{13}$, $\gamma_2 = \gamma_3 = 10^8$, $\gamma_{ab} = 10^{-10}e$-cm, $N_a = 10^{23}\,\mathrm{cm}^{-3}$. (a) $E_{Control} = 10^{13}\,\mathrm{Vm}^{-1}$, (b) $E_{Control} = 1.5 \times 10^{13}\,\mathrm{Vm}^{-1}$, (c) $E_{Control} = 2.5 \times 10^{13}\,\mathrm{Vm}^{-1}$.

Considering the illustrated figures, it is observed that with increasing of the control field the oscillatory part of the transmission coefficient is extended to large wavelength duration.

Until now it is observed that with considering EIT case the resolution of the presented optical displacement sensor is increased. Well below nanometer measurement in this case is possible. The

presented method, which can be realized using Si nanocrystals doped in basic silica ring resonators, can operate as basic method for implementation of all-optical sub-nanometer displacement sensor.

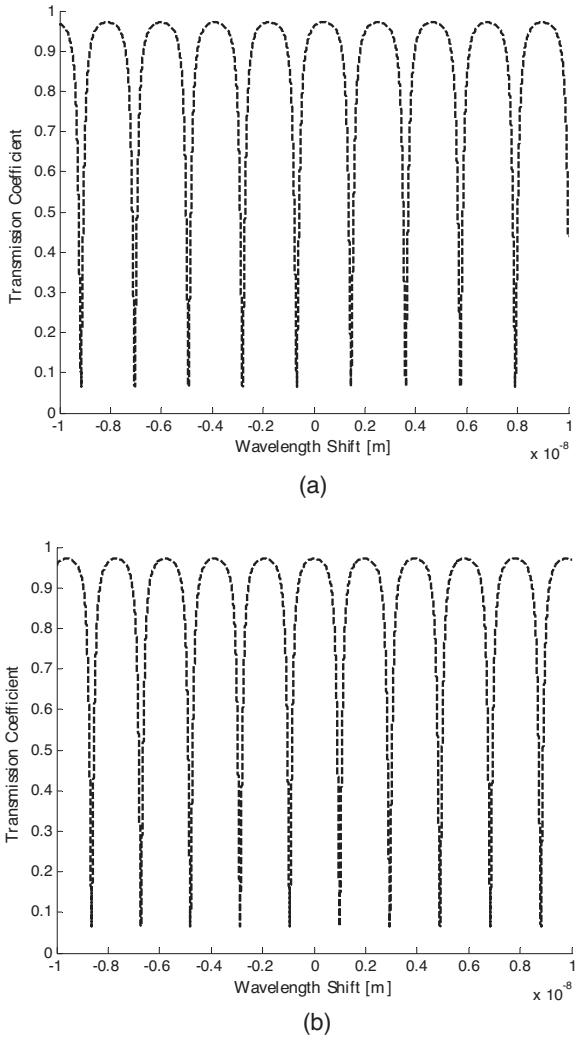

Figure 7. Transmission coefficient Vs. wavelength for optical displacement sensor based on ring resonator. $L_{23} = L_{45} = 248\,\mu$m, $h = 5\,\mu$m, $K_1 = 0.4$, $\lambda_0 = 1.55\,\mu$m, $r = 0.8$, $\gamma_1 = 10^{-3}\,\mathrm{m}^{-1}$, $\alpha = 10^{-3}\,\mathrm{m}^{-1}$, $\alpha_0 = 0.1\,\mathrm{m}^{-1}$. (a) $\Delta x = 1\,\mu$m, (b) $\Delta x = 5\,\mu$m.

In the following simulations, we investigate effect of length of ring resonator on sensitivity of the designed sensor. Fig. 7 shows the transmission coefficient of displacement sensor in normal case. It is observed that with increasing the ring length the transmission coefficient is changed sharply and the period of oscillation in wavelength domain is decreased. It is observed that with increasing displacement the resonance frequency is increased.

Figure 8 typically shows effect of large ring length on the transmission coefficient for both EIT and normal cases.

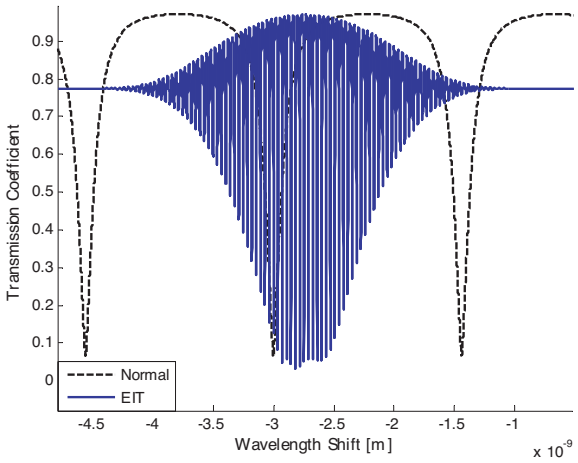

Figure 8. Transmission coefficient Vs. wavelength for normal and EIT cases. $L_{23} = L_{45} = 248\,\mu$m, $h = 5\,\mu$m, $\Delta x = 15\,\mu$m, $K_1 = 0.4$, $\lambda_0 = 1.55\,\mu$m, $r = 0.8$, $\gamma_1 = 10^{-3}\,\mathrm{m}^{-1}$, $\alpha = 10^{-3}\,\mathrm{m}^{-1}$, $\alpha_0 = 0.1\,\mathrm{m}^{-1}$, $E_{Control} = 2.5 \times 10^{13}\,\mathrm{Vm}^{-1}$, $\gamma_1 = 10^{13}$, $\gamma_2 = \gamma_3 = 10^8$, $\gamma_{ab} = 10^{-10}$*e*-cm, $N_a = 10^{23}\,\mathrm{cm}^{-3}$.

In the following optical susceptibility (real and imaginary parts) versus wavelength for large ring length and given displacement is illustrated. Also, the control field is changed and result is illustrated. It is observed that with increasing the control field the imaginary part shows transparency in wider range of wavelength and the slope of the real part is decreased.

In the following effect of the control field on the transmission coefficient is investigated. It is observed that with increasing the control field in this case the oscillatory section is extended too. Also, the filtering property of the proposed structure is observed in this case which is so narrower than previous cases.

As a final set of figures illustrating ability of the proposed sensor in the following, we illustrate the wavelength displacement versus displacement of object. It is observed that in the case of EIT the wavelength displacement from off to on position of the output intensity that is measurable quantity in practice is so smaller than normal case. On the other hand sensitivity of the EIT case can be increased using applied control field and well over 200 times the precision can be increased.

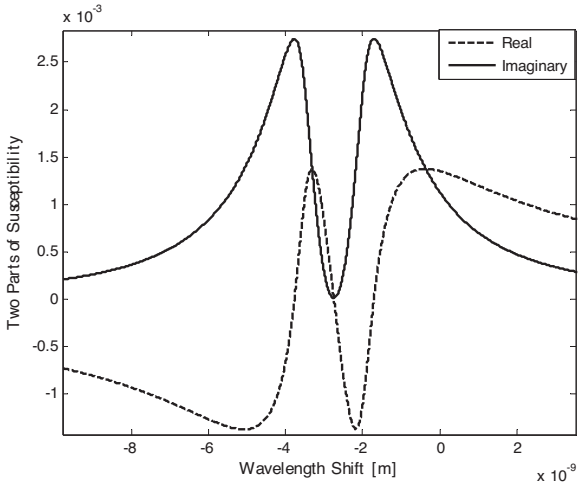

(a)

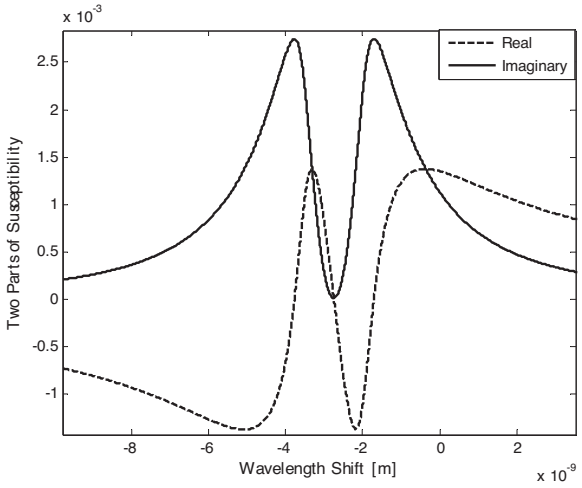

(b)

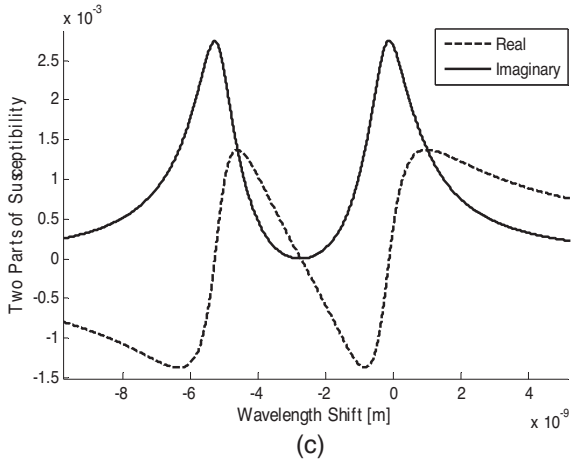

Figure 9. Real and imaginary parts of optical susceptibility Vs. wavelength. $L_{23} = L_{45} = 248\,\mu$m, $h = 5\,\mu$m, $\Delta x = 1\,\mu$m, $K_1 = 0.4$, $\lambda_0 = 1.55\,\mu$m, $r = 0.8$, $\gamma_1 = 10^{-3}\,\mathrm{m}^{-1}$, $\alpha = 10^{-3}\,\mathrm{m}^{-1}$, $\alpha_0 = 0.1\,\mathrm{m}^{-1}$, $\gamma_1 = 10^{13}$, $\gamma_2 = \gamma_3 = 10^8$, $\gamma_{ab} = 10^{-10}e$-cm, $N_a = 10^{23}\,\mathrm{cm}^{-3}$. (a) $E_{Control} = 10^{13}\,\mathrm{Vm}^{-1}$, (b) $E_{Control} = 1.5 \times 10^{13}\,\mathrm{Vm}^{-1}$, (c) $E_{Control} = 2.5 \times 10^{13}\,\mathrm{Vm}^{-1}$.

Finally effect of displacement on the transmission coefficient for different displacement values in both normal and EIT cases are illustrated in Fig. 12. It is shown that the EIT case is so sensitive

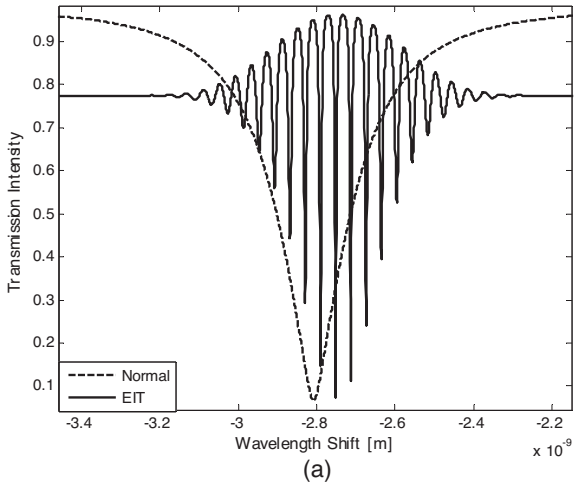

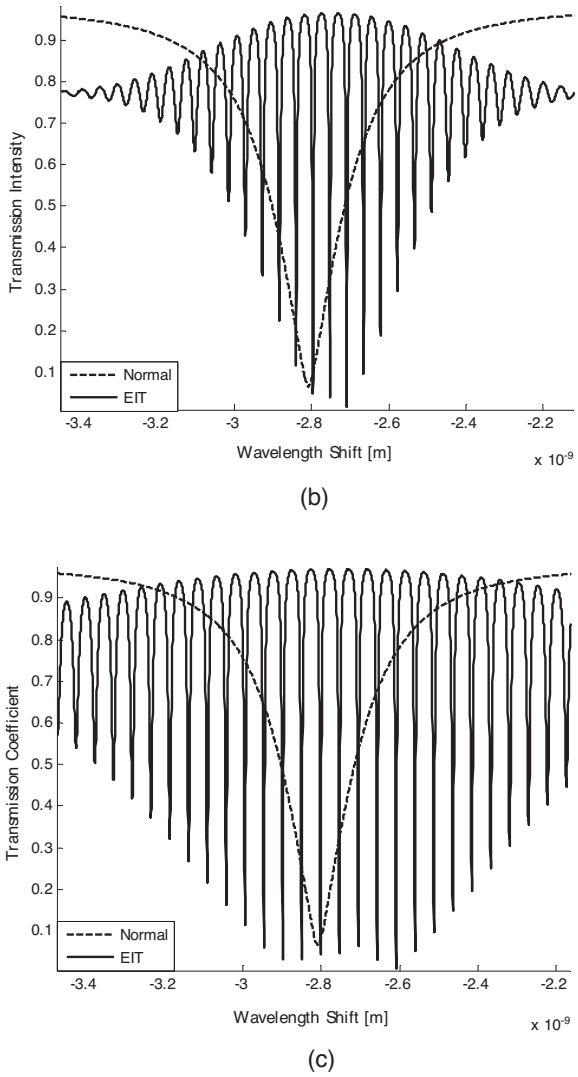

Figure 10. Transmission coefficient Vs. wavelength for normal and EIT cases. $L_{23} = L_{45} = 248\,\mu$m, $h = 5\mu$m, $\Delta x = 1\mu$m, $K_1 = 0.4$, $\lambda_0 = 1.55\,\mu$m, $r = 0.8$, $\gamma_1 = 10^{-3}\,\mathrm{m}^{-1}$, $\alpha = 10^{-3}\,\mathrm{m}^{-1}$, $\alpha_0 = 0.1\,\mathrm{m}^{-1}$, $\gamma_1 = 10^{13}$, $\gamma_2 = \gamma_3 = 10^8$, $\gamma_{ab} = 10^{-10}e$-cm, $N_a = 10^{23}\,\mathrm{cm}^{-3}$. (a) $E_{Control} = 10^{13}\,\mathrm{Vm}^{-1}$, (b) $E_{Control} = 1.5 \times 10^{13}\,\mathrm{Vm}^{-1}$, (c) $E_{Control} = 2.5 \times 10^{13}\,\mathrm{Vm}^{-1}$.

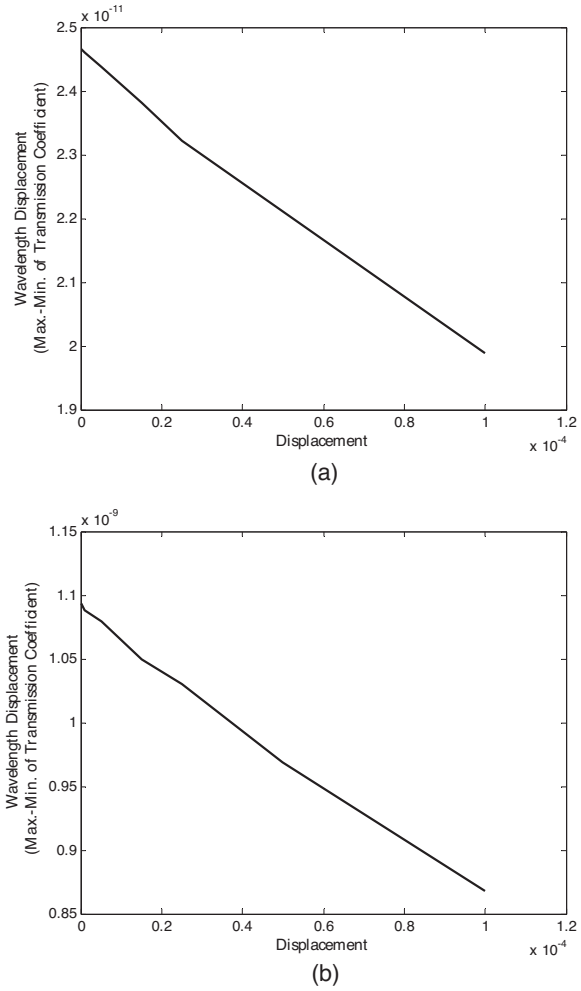

Figure 11. Wavelength displacement Vs. displacement in EIT (a) and Normal (b) Cases.

compared normal case.

In this section effect of 3-level particles on the reflection coefficient of the proposed system for displacement sensor was investigated. It was shown that in the proposed case ultra-high precision displacement detection is possible.

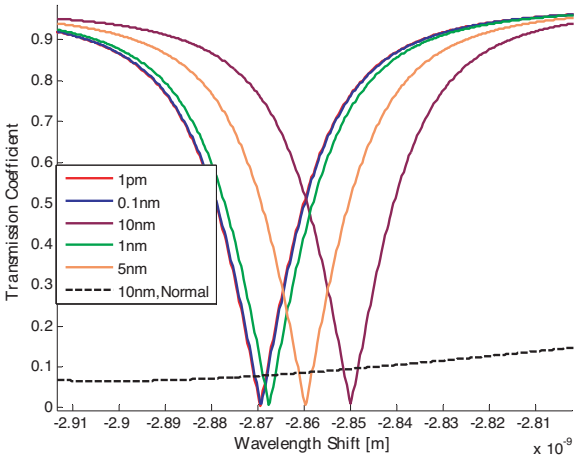

Figure 12. Wavelength displacement Vs. displacement in EIT and Normal Cases for different displacements.

4. CONCLUSION

In this paper a novel and ultra-high precision optical displacement sensor using electromagnetically induced transparency (EIT) in micro-ring resonator has been presented. It was shown that the proposed method introduces well over 200 times better resolution than normal cases. Effects of different system parameters on operation and sensor sensitivity have been considered and evaluated.

REFERENCES

1. Webster, J. G., *Measurement, Instrumentation, and Sensors Handbook*, CRC Press LLC, 2003.
2. Dandridge A., *Fiber Optic Sensors Based on the Mach-Zehnder and Michelson Interferometers, in Fiber Optic Sensors: An Introduction for Engineers and Scientists*, Wiley, New York, 1991.
3. Kersey, A. D., "Distributed and multiplexed fiber optic sensors," *Fiber Optic Sensors: An Introduction for Engineers and Scientists*, Wiley, New York, 1991.
4. Marcuse, D., *Principles of Optical Fiber Measurements*, Academic Press, New York, 1981.
5. Vollmer, F. and P. Fischer, "Frequency-domain displacement

sensing with a fiber ring-resonator," *Sensors and Actuators A*, Vol. 134, 410–413, 2007.

6. Rostami, A. and G. Rostami, "Full optical analog to digital (A/D) converter based on Kerr-like nonlinear ring resonator," *Optics Communications*, Vol. 228, 39–48, 2003.
7. Rostami, A. and K. Abbasian, "All-optical filter design: electromagnetically induced transparency and ring resonator," *Proceeding of ICT-MICC 2007*, Malaysia, Penang, 2007.
8. Kiyat, I., C. Kocabas, and A. Aydinli, "Integrated microring resonator displacement sensor for scanning probe microscopes," *J. Micromechanical MicroEng.*, Vol. 14, 374–387, 2004.
9. White, I. M., H. Zhu, J. D. Suter, H. Oveys, and X. Fan, "Liquid core optical ring resonator sensors," *Optics Letters*, Vol. 31, 1319–1321, 2006.
10. Boyd, R. W. and J. E. Heebner, "Sensitive disk resonator photonic biosensor," *Appl. Opt.*, Vol. 40, 5742–5747, 2001.
11. Lee, H., M. Fleischhauer, and M. O. Scully, "Sensitive detection of magnetic fields including their orientation with a magnetometer based on atomic phase coherence," *Phys. Rev. A*, Vol. 58, No. 3, 1998.
12. Host, C. M. K., "Design and modeling of waveguide coupled single mode microring resonators," *J. Lightwave Technology*, Vol. 16, 1433–1446, 1998.
13. Okamura, H. and K. Iwatsuki, "A finesse-enhanced Er doped fiber ring resonator," *J. Lightwave Technology*, Vol. 9, 1557–1560, 1991.
14. Agrawal, G. P., *Fiber Optic Communication Systems*, John Wiley & Sons, Inc., 2002.
15. Agrawal, G. P., *Nonlinear Fiber Optics*, Academic Press, 2001.
16. Suh, W., O. Solgaard, and S. Fan, "Displacement sensing using evanescent tunneling between guided resonances in photonic crystal slabs," *J. of Applied Physics*, Vol. 98, 033102, 2005.
17. Lopez, J. M., *Handbook of Optical Fiber Sensing Technology*, Wiley, Chichester, 2002.
18. Chen, H., L. X. Ran, J. Huangfu, X. M. Zhang, K. S. Cheng, T. M. Grzegorczyk, and J. A. Kong, "Magnetic properties of S-shaped split-ring resonators," *Progress In Electromagnetics Research*, PIER 51, 231–247, 2005.
19. Lee, S. W., W. Kuga, and A. Ishimaru, "Quasi-static analysis of materials with small tunable stacked split ring resonators," *Progress In Electromagnetics Research*, PIER 51, 219–229, 2005.
20. Yao, H. Y., L. W. Li, Q. Wu, and J. A. Kong, "Macroscopic per-

formance analysis of metamaterials synthesized from microscopic 2-D isotropic cross split-ring resonator array," *Progress In Electromagnetics Research*, PIER 51, 197–217, 2005.

21. Zhang, J., B. Cui, S. Lin, and X. W. Sun, "Sharp-rejection low-pass filter with controllable transmission zero using complementary split ring resonators (CSRRs)," *Progress In Electromagnetics Research*, PIER 69, 219–226, 2007.
22. Zhang, X. C., Z. Y. Yu, and J. Xu, "Novel band-pass substrate integrated waveguide (SIW) filter based on complementary split ring resonators (CSRRs)," *Progress In Electromagnetics Research*, PIER 72, 39–46, 2007.
23. Fan, J. W., C. H. Liang, and X. W. Dai, "Design of cross-coupled dual-band filter with equal-length split-ring resonators," *Progress In Electromagnetics Research*, PIER 75, 285–293, 2007.
24. Niu, J. X., X. L. Zhou, and L. S. Wu, "Analysis and application of novel structures based on split ring resonators and coupled lines," *Progress In Electromagnetics Research*, PIER 75, 153–162, 2007.
25. Scully, M. O. and M. S. Zubairy, *Quantum Optics*, Cambridge University Press, 1997.